Parameter optimization for fusion neutron yield from deuterium cluster explosion driven by intense femtosecond laser pulses

Hongyu Li,[1,*] Jiansheng Liu,[2] Guoquan Ni,[2] Ruxin Li,[2] and Zhizhan Xu[2,†]

[1]*College of Physics and Electronic Information, Tianjin Normal University, Tianjin 300387, People's Republic of China*

[2]*State Key Laboratory of High Field Laser Physics, Shanghai Institute of Optics and Fine Mechanics, Chinese Academy of Sciences, P.O. Box 800-211, Shanghai 201800, People's Republic of China*

(Received 27 October 2008; revised manuscript received 7 March 2009; published 16 April 2009)

A modified model based on the Coulomb explosion model [H. Li *et al.*, Phys. Rev. A **74**, 023201 (2006)] is proposed to roughly estimate the nuclear fusion yields produced in the Coulomb explosion of deuterium cluster jet with irradiation of the intense laser pulses by taking the attenuation of laser energy absorbed by the clusters with a logarithmic-normal size distribution into account. The neutron yield generated inside the heated plasma filament, as the sum of the intercluster fusion yield and beam-target fusion yield, is calculated as a function of laser-cluster parameters such as the cluster size, the laser energy, and the focus spot radius and position. Only if these parameters match with each other can the neutron yield or the neutron conversion efficiency be maximized. The rough qualitative comparison about the variation tendency of fusion yield with laser-cluster parameters is made between our simulations and the reported measurements.

DOI: 10.1103/PhysRevA.79.043204 PACS number(s): 36.40.Wa, 36.40.Qv, 52.50.Jm, 25.45.−z

I. INTRODUCTION

As bridge state from atoms to bulk solid, clusters with large sizes irradiated by intense laser pulses higher than 10^{15} W/cm^2 can generate MeV ions [1–6] and intense x rays [7–10], which has contributed to the investigation of laser-induced nuclear fusion and table-top x-ray laser, etc. In a series of important experiments of the Lawrence Livermore group [11–15], ultrashort laser pulses with high intensity are focused into the deuterium cluster $(D_2)_n$ jet to heat the clusters rapidly. Then the clusters explode outwards with the generation of high-energy deuterons, forming a hot plasma filament with a diameter determined by the laser focus spot and with a length dependent on the absorption depth of the laser pulse into the cluster gas. Generally, the D-D fusion neutron production in the cluster explosion process includes contributions from the collisions among the energetic deuterons produced in different clusters inside the cluster plasma, termed as intercluster fusion [16], as well as from the collisions of hot deuterons streaming out the plasma with cold deuterium atoms in the surrounding gas, termed as beam-target fusion [17,18]. Apart from the above two fusion mechanisms, another possible D-D nuclear fusion mechanism is the collision and fusion between the hot deuterons within a single cluster, termed as intracluster fusion [19–22]. The intracluster fusion depends greatly on the formation of shock shells resulting from the nonuniform density profiles inside the single cluster in the early period of the Coulomb explosion and thus happens in a smaller spatial scale of a few cluster radius and an earlier temporal scale than the intercluster fusion event. However, it is still an open question whether the shock shells originating from the density nonuniform in the Coulomb explosion of homonucluster clusters can be realized [22]. Even if it were realized, only when the shock shells are great enough can the intracluster fusion yield be comparable to the intercluster fusion yield [21]. For heteronuclear clusters, the possible intracluster nucleosynthesis fusion happens when some parts of light ions overtake the heavy ions due to the kinetic overrun effects [23–25]. Particularly in the exploding process of a deuterated heteronuclear cluster such as $(DI)_n$, if the deuterons on the inner layers had large velocity to overrun not only the heavy ions on the outer layers but also the periphery deuterons, a narrow shock shell forms where the D-D nuclear fusions might occur between the deuterons moving with large relative velocities in the same direction. It is unfortunate that the neutron yield produced in the intracluster fusion model is still much lower than the intercluster fusion yield due to the small scale of the shock shells [26].

Researchers have made systematic experiments [12,15,17,27,28] and established reasonable models [29–37] to investigate the neutron production in the Coulomb explosion processes of the deuterated clusters driven by ultraintense femtosecond laser beams. Some useful scaling laws have been obtained, e.g., the neutron yields from the laser-heated homonuclear deuterium clusters and heteronuclear clusters containing deuterium are highly affected by the cluster size as well as the laser-pulse characteristic parameters. Meanwhile, the effect of the cluster size distributions on the theoretical and experimental studies about the cluster dynamics in ultraintense laser fields is being realized [38–41]. In view of the very efficient laser energy absorption by clusters [1,12,14,17,33], the laser light intensity attenuation in the propagation process of the laser beams within the cluster jet should also be considered, especially when the numerical simulations are compared with the measurements. For example, by use of classical dynamics simulations, Last and Jortner [37] discussed the effects of the laser intensity attenuation due to absorption by an assembly of homonuclear deuterium clusters in the cluster vertical ionization (CVI) domain and in the non-CVI domain. However, just limited by the simulation method it is relatively difficult to consider the

*hongyuli79@gmail.com

†zzxu@mail.shcnc.ac.cn

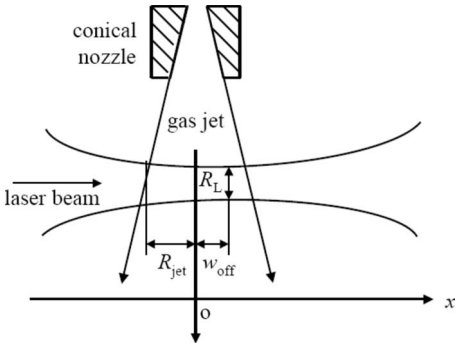

FIG. 1. The geometry structure design of the intense laser beam interacting with the cluster jet flow. The parameters characterizing the laser focal volume and the cluster jet are also indicated in this figure. As an example, the Gaussian laser pulse is focused on the back of the cluster filament and thus the laser focus position w_{off} has a plus value at the x axis.

influence of cluster size distribution in their studies since the inclusion of cluster size distribution means considerable calculation efforts [29–32]. Relative to the many experimental scaling results of the neutron yield with the laser-cluster parameters and the various theoretical simulations about the cluster dynamics process including some key factors, the theoretical systematic analyses of the neutron production for relevant parameters integrating the cluster size distribution and the attenuation of the laser energy absorbed by clusters are still lacking. In this paper we aim to employ the relatively simplified and effective numerical simulations incorporating the effects of the laser energy attenuation and the cluster size distribution to obtain the optimum relations of the laser and deuterium cluster parameters that determine the neutron yield maximization. These relations will supply the possible theoretical reference for further establishing experimental schemes.

II. CALCULATING MODEL FOR LASER-HEATED DEUTERIUM CLUSTER FUSION YIELDS

Taking the attenuation of laser energy absorbed by clusters into account, a model is proposed herein to study the nuclear fusions inside the generated hot plasma filament when the intense laser pulses heat up the deuterium cluster jet with a logarithmic-normal cluster size distribution [38]. The geometry structure design of the intense laser beam interacting with the cluster jet flow is plotted in Fig. 1, same as described in Ref. [42]. In our model, the cluster gas jet is approximated to have a uniform density and have a conical spatial profile due to the cluster formation process output from the conical nozzle, while the laser beam is assumed to be Gaussian with a Rayleigh length

$$Z_R = \pi R_L^2/\lambda, \tag{1}$$

where R_L is the waist radius of the Gaussian laser beam and λ is the laser center wavelength. Setting the horizontal coordinate along the laser propagation direction as the x axis and the cross point between the laser beam and the center line of the the gas flow as the origin, the laser beam radius R_x as a function of x can be expressed as

$$R_x = R_L\sqrt{1+[(x-w_{off})/Z_R]^2}, \tag{2}$$

where w_{off} is the laser focus position at the x axis. It should be pointed out that when the laser-pulse beam propagating through the dense jet, its profile is expected to be modified because of two relative but opposite effects, i.e., the defocusing effect induced by the gas ionization [43–45] and the self-focusing related to the cluster ionization [46–48]. In particular conditions [42], the two effects on the laser shape can be neglected, i.e., the laser intensity along the propagation axis through the cluster jet keeps as a Gaussian shape similar to the case in vacuum. On the above assumption, the interaction volume can be defined as the intersection space of the Gaussian laser beam and the conical gas flow and be divided into a series of cylindrical segments with radius R_x along the x axis. In each segment of volume $dV=\pi R_r^2 dx$, the laser intensity is considered to be constant and defined as

$$I(x) = E_L(x)/\pi R_x^2\tau, \tag{3}$$

where E_L is the laser energy in the segment and τ is the laser-pulse temporal width.

At the early phase of an ultraintense laser-pulse irradiating gas clusters, the atoms or molecules inside the clusters are ionized by the optical field and converted into charged ions and free electrons. The laser strips the generated free electrons off the cluster, driving the cluster to explode outwards. In this way, the laser energy is partly attenuated because of the absorption by the clusters. The energy loss is transferred into the ionization energy of the atoms or molecules in clusters, the final kinetic energy of ionized electrons, and the final kinetic energy of atomic particles (ions or nuclei). The theoretical calculations of Last and Jortner [37] indicated that for extreme ionization of atomic or molecular clusters consisting of many-electron atoms, e.g., $(Xe)_n$ or $(CD_4)_n$, the ionization energy is relatively higher and has to be included in the transferred energy loss; while for the few-electron atom clusters, e.g., $(D_2)_n$, the ionization energy is considerably lower than the deuteron energy and can be neglected in the absorbed laser energy. Furthermore, on the basis of molecular-dynamics simulations, they obtained an analytical expression to fit the relation between the energy $E^{(p)}$ absorbed by a deuterium cluster with radius R_0 and the final kinetic energy $E^{(a)}$ of all ions in the cluster,

$$E^{(p)} = \{1.15 + 0.68/[1+(R_0/R_0^{(I)})^2]\}E^{(a)}. \tag{4}$$

In this expression, the upper border $R_0^{(I)}$ of the cluster which can realize the CVI [49] is represented by the empirical relation

$$R_0^{(I)}(\text{Å}) = 2.65\times 10^{-8}[\tau(\text{fs})]^{0.62}[I_M(\text{W/cm}^2)]^{1/2}. \tag{5}$$

It can be concluded from Eq. (4) that the ratio of $E^{(p)}$ to $E^{(a)}$ is in the interval of 1.15–1.83. Only for the cluster with $R_0 \ll R_0^{(I)}$ under high intensity laser, the CVI and the pure Coulomb explosion (PCE) [41] make the ratio close to 1.83. While in the "cold" nanoplasma domain, the ratio is saturated at 1.15 under the relation of $R_0^{(I)} \ll R_0$. Parks *et al.* [33]obtained the ratio of $E^{(p)}/E^{(a)} \approx 1.47$ by using their proposed model, and Eloy *et al.* [50] found a ratio value of 1.8 with the full relativistic particle-in-cell code. Their results

are also in the quantitative domain of Eq. (4).

The electrostatic Coulomb explosion model proposed by us in another paper [41] is also used here to simulate the interaction process of the laser with one deuterium cluster and to obtain the kinetic energy of all deuterons in a cluster. Then the absorbed energy by one cluster can be calculated by Eq. (4). To obtain the deuteron energy distribution and the total-energy loss of the laser when it passes each individual segment of the interaction volume, a logarithmic-normal cluster size distribution is also considered with the definition

$$f(N_c) \propto \exp[-\ln^2(N_c/N_M)/2w^2], \tag{6}$$

where N_M is the modal cluster size and w is proportional to the full width half maximum of the distribution [38]. The width of the distribution is assumed approximately equal to N_M and thus w is 0.4087, accordingly. The mean cluster size $\bar{N}$ relates to N_M by $N_M=\bar{N}/1.29$ and to the mean cluster radius R_0 by $\bar{N}=4\pi R_0^3\rho_0/3$, where $\rho_0=3\times10^{22}/\mathrm{cm}^3$ [12] is the local atomic density of the deuterium cluster.

The neutron yields of the intercluster fusion and beam-target fusion can be roughly estimated as [26]

$$Y_{\mathrm{IC}}=\frac{1}{2}\bar{\rho}^2 L_{\mathrm{IC}} V_r \langle\sigma\rangle_{\mathrm{IC}} \quad \text{and} \quad Y_{\mathrm{BT}}=\bar{\rho}^2 L_{\mathrm{BT}} V_r \langle\sigma\rangle_{\mathrm{BT}}. \tag{7}$$

In this expression, $V_r=\pi\bar{R}_r^2 H_r$ is the volume of the heated cluster plasma cylinder with a radius of $\bar{R}_r$ and a height of H_r. The cylinder radius $\bar{R}_r$ is taken to be the average value of the varying laser beam radius R_x along the laser propagation axis. L_{IC} is a characteristic distance free streaming ions will traverse inside the cluster plasma and can be estimated as the cylinder diameter, i.e., $L_{\mathrm{IC}}=2\bar{R}_r$. L_{BT} is the characteristic distance free ions will traverse when streaming from the cluster plasma into the surrounding cold gas and is comparable to the radius of the gas jet, i.e., $L_{\mathrm{BT}}=2R_{\mathrm{jet}}$. $\bar{\rho}$ is the average number density of nuclei inside the heated cluster plasma with the typical value of $2\times10^{19}/\mathrm{cm}^3$ [13]. $\langle\sigma\rangle$ is the averaged fusion cross section with the same definition as that in Ref. [26].Our simulating calculations indicate that for the chosen laser-cluster parameters in this paper, the laser beam can penetrate through the cluster jet because of the high initial laser energy, still with the efficient energy absorption by the clusters. Some cases as examples with different parameters are shown in Fig. 2. In this figure, the absorption efficiency of the laser energy is calculated with the definition of the remained energy of the laser beam when it passes by the cluster jet divided by the initial laser energy. The attenuation effect is included in all the following calculations and due to the above reasons the whole interaction volume is estimated as the cluster plasma cylinder with the same length of $H_r=2R_{\mathrm{jet}}$, where R_{jet} is the radius of cluster jet taken to be 2 mm at general experimental condition referring to Refs. [13,14].

In our calculation, the intracluster fusion is ignored since the deuterium clusters are assumed with initial uniform density. The neutron yield Y presented in the next context is defined as the sum of the intercluster fusion yield Y_{IC} and beam-target fusion yield Y_{BT}. The conclusion obtained in Ref. [26] presented that with the deuteron energy increasing, Y_{IC} and Y_{BT} will increase and finally Y_{BT} will exceed Y_{IC}.

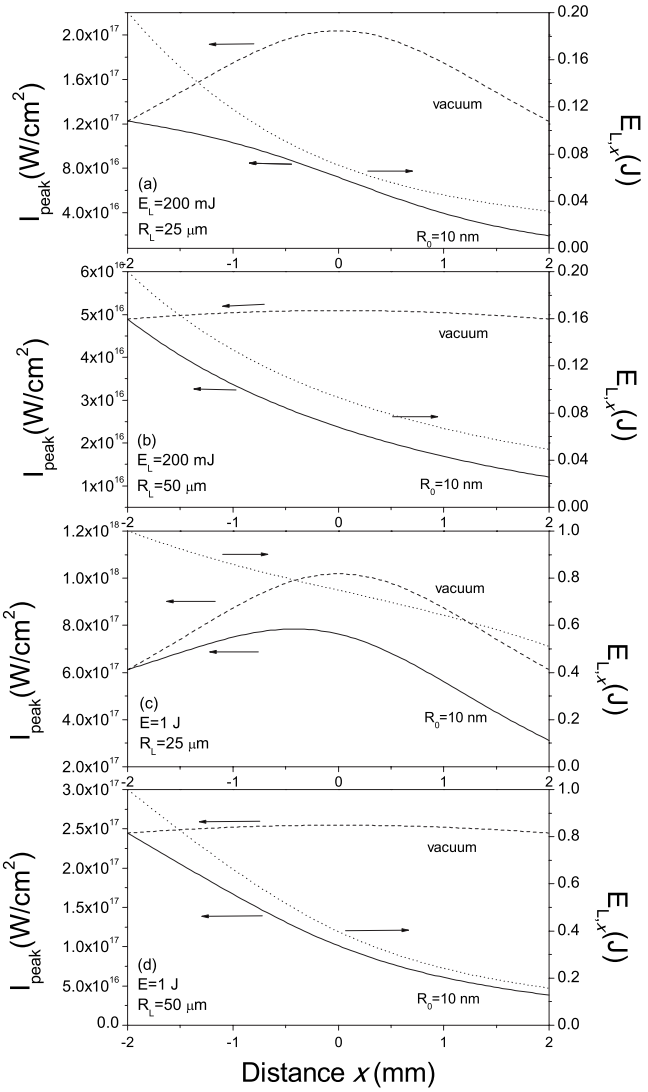

FIG. 2. The distribution of the laser peak intensity I_{peak} and of the laser energy $E_{L,x}$ at distance x along the propagation axis. The dash lines and the solid lines represent the laser intensity distribution when the laser pulse propagates in the vacuum and in the cluster jet, respectively. The dot lines represent the laser energy distribution when the laser propagates in the cluster jet and the calculated absorption efficiency of the laser energy is (a) 84%, (b) 75%, (c) 49%, and (d) 84%. The laser pulse (50 fs, 800 nm) is focused to the center of cluster flow with the radius $R_{\mathrm{jet}}=2$ mm. The clusters are assumed with the average cluster radius of $R_0=10$ nm and the size distribution width $w=0.4087$, while the local atomic density ρ_0 of the deuterium cluster and the average number density $\bar{\rho}$ of nuclei inside the cluster filament are taken as 3×10^{22} and $2\times10^{19}/\mathrm{cm}^3$, respectively.

III. DEPENDENCE OF FUSION YIELD ON LASER-CLUSTER PARAMETERS

A. Dependence of fusion yield on laser focus radius

The scalings of the fusion neutron yield Y and the yield per joule of incident laser energy $Y/E_L(\mathrm{J}^{-1})$ with the laser

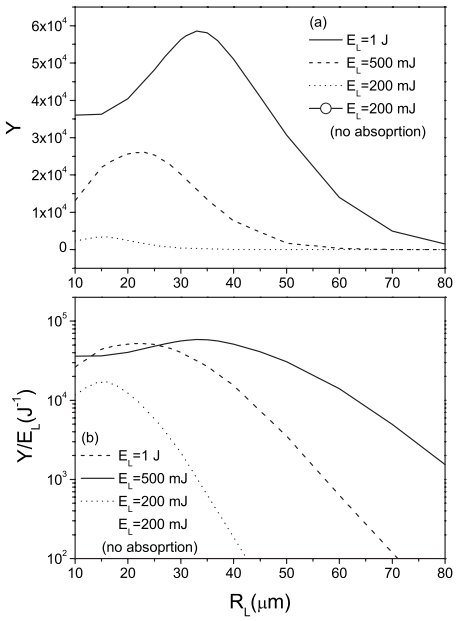

FIG. 3. Scalings of (a) the fusion neutron yield Y and (b) the yield per joule of incident laser energy $Y/E_L(\mathrm{J}^{-1})$ with the laser focus radius R_L for different laser energies E_L. The mean cluster radius R_0 is about 10 nm and the laser focus is located at the cluster jet center. As an elementary reference situation, the dependence of neutron yield with the laser focus radius when the attenuation effect is absent for the laser energy $E_L=200$ mJ is plotted with open circles.

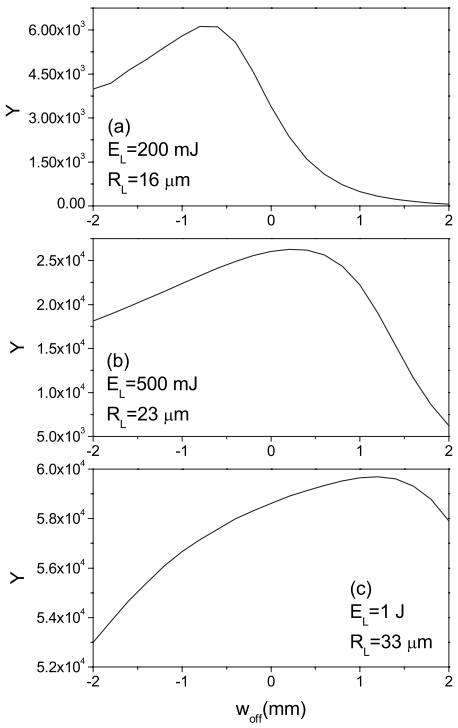

FIG. 4. Fusion yield Y as a function of laser focus position w_{off} at the x axis for varying initial laser energy E_L and focus radius R_L. The mean cluster radius R_0 is about 10 nm.

focus radius R_L for different laser energies E_L have been calculated as presented in Figs. 3(a) and 3(b), respectively. The comparison between the dot line and the open circles in Fig. 3(a) shows that when the initial laser energy $E_L=200$ mJ and the focus position at the cluster jet center are kept unchanged, the calculated neutron yield for every focus radius R_L with the attenuation effect originating from the laser energy absorption by the cluster jet is lowered by almost 1 order of magnitude than the yield without the attenuation effect. The influence of the laser energy loss due to the clusters absorption on the fusion yield is so great that it must be considered in the accurate discussion about the neutron yield with variable laser-cluster parameters. Moreover it is shown from Fig. 3(a) that for the same initial laser energy and focus position, with the laser focus radius broadening the neutron yield increases until it reaches a peak value, after which point the yield decreases slowly towards zero. The reason is that for a given laser energy, when the laser focus spot becomes smaller, the laser intensity will grow higher to make the majority of the clusters in the jet finish the outer ionization earlier and faster. In this way, the deuterons gain higher energy and the averaged fusion cross section becomes larger. From this viewpoint, the decreasing laser focus radius has a positive effect on the improvement of the fusion yield. On the other hand, as a result of the laser spot size decreasing, the reduced number of the deuterium ions in the plasma filament has a negative effect on the increase in the fusion yield. The competition between the two effects makes the relation of fusion yield to the focus radius nonlinear and then an optimum focus radius exists corresponding to the maximum fusion yield. This relationship is qualitatively in agreement with the conclusion reported in Ref. [36].

Moreover, the curves illustrated in Fig. 3(b) shows that an optimum focus radius exists to maximize the neutron yield per joule of incident laser energy for the given laser energy and focus position. The fusion yield per joule of incident laser energy represents the conversion efficiency of the laser energy transferring to the neutron yield. For the parameters chosen here, the higher the laser energy is, the larger the optimum focus radius is allowed for higher fusion yield per joule of incident laser energy, which means the laser energy is transferred more effectively to the deuterons energy.

B. Scaling of fusion yield with focus position

According to the parameter optimum relation shown in Fig. 3, when the focus position of a laser with certain energy is near to the center of the cluster jet, the focus radius maximizing the neutron yield is defined as the optimum focus radius. For example, the optimum focus radii for the laser energy of 200 mJ, 500 mJ, and 1 J are 16 μm, 23 μm, and 33 μm, respectively. Keeping the optimum radius for the particular laser energy invariable, we plot the dependence of the fusion yield Y on the laser focus position w_{off} at the x axis in Fig. 4. As the focus position moves backwards along the laser propagation direction, the yield rises to a peak and then falls down. This trend of the fusion yield with the focus position is similar with the experiment scaling law reported in Fig. 8 of Ref. [15]. The difference is that in their report as the laser energy is varied, the peak yield rests at the same focus position; however, our calculation indicates that the

optimum focus position appears to move around with the varying laser energy. It is because, to maximize the fusion yield, the focus radius is adjusted as the optimum focus radius according to the different laser energy in our investigation while the focus radius chosen for discussing the relation has not been changed in Ref. [15].

When the initial laser energies are 200 and 500 mJ, respectively, the focus position has an important effect on the fusion yield. As the laser energy is 1 J, the yield varies in a narrow magnitude of 5.2×10^4–6×10^4 with the changing focus position, i.e., the focus position has an ignorable influence on the fusion yield. Our simulation shows that the laser beam can penetrate through the cluster jet for the different laser and cluster parameters chosen here so that the generated cluster filament cylinders have the same length equal to the cluster jet diameter of $2R_{\mathrm{jet}}=4$ mm. When the laser focus radii are 16, 23, and 33 μm, the corresponding Rayleigh lengths are 1.01, 2.07, and 4.28 mm, respectively. If the Gaussian laser pulse with focus radius of 16 μm is focused on the front port of the cluster filament (i.e., $w_{\mathrm{off}}=-R_{\mathrm{jet}}$), the maximum laser spot radius along the laser propagation axis locates to the back port of the cluster jet and is about 4.08 R_L according to the definition of Eq. (2). For the case that the laser pulse with the same focus radius is focused on the center of the cluster jet (i.e., $w_{\mathrm{off}}=0$), the maximum laser spot radius in the cluster filament is 2.22 R_L. The ratio of the two laser spot radius maximums is $4.08/2.22=1.84$. (Note: when the laser is focused on the back port of the cluster jet, the maximum laser spot radius has the same value as that of the laser focused on the front port of the cluster jet.) In another case of the focus radius equal to 23 μm, the ratio of the spot radius maximum when the laser is focused to the cluster jet front port to that of the laser being focused on the jet center is $2.18/1.39=1.57$, which indicates the changing range of the laser spot radius along the laser propagation axis originating from the varied laser focus position is also large but lower than that of focus radius 16 μm. If the focus radius is 33 μm, the ratio is $1.37/1.10=1.25$, meaning the laser spot radius along the laser propagation changes in a small scale. The smaller the focus radius is, the more intensely the laser spot radius along the propagation axis changes and more distinct the influence of the focus position on the focus radius variation is. Therefore, both the laser intensity along the axis and the volume of the filament change in a more violent range, and the two factors will effect the absorption of laser energy by the clusters in the filament, finally leading to the greater difference of fusion neutron yield, which is plotted in Figs. 4(a) and 4(b), respectively. However, if the laser focus radius is relatively larger, e.g., 33 μm, the laser intensity as well as the filament volume change a little when the laser beam propagates in the cluster jet, and therefore the neutron yield is not sensitive to the difference of the focus positions, which is shown in Fig. 4(c).

C. Dependence of fusion yield on pulse energy

Keeping the focus position at the cluster jet center and the focus radius to be constant, the fusion yields versus initial laser energy are illustrated in Fig. 5. As shown with solid circles in Fig. 5(a), for the focus radius of 50 μm, the laser energy less than 300 mJ only produces very low neutron yield. It results from that the laser pulse with lower energy only can strip a small part of electrons off the clusters to acquire lower deuteron energy and then lower neutron yield. As the laser energy grows higher than 300 mJ, the fusion yield increases sharply, and then the increasing trend slows down when the laser energy become higher than 2 J after which point the yield begins to fall down. The reason for the yield saturation is that clusters with different sizes have already realized the approximately pure Coulomb explosion under the irradiation of the high intense laser and the deuteron energies have approached to saturation. This relation can be confirmed by the scaling of the neutron yield per joule of incident laser energy $Y/E_L(\mathrm{J}^{-1})$ with the increasing laser energy, which is represented by open circles in Fig. 5. As the laser energy increases, Y/E_L firstly increases fast which means the conversion ratio of the laser energy transferring to the neutron yield is increased. However, when the fusion yield Y tends to saturate the laser energy cannot effectively enhance the neutron yield even if it continues to rise so that the conversion efficiency appears to decrease.

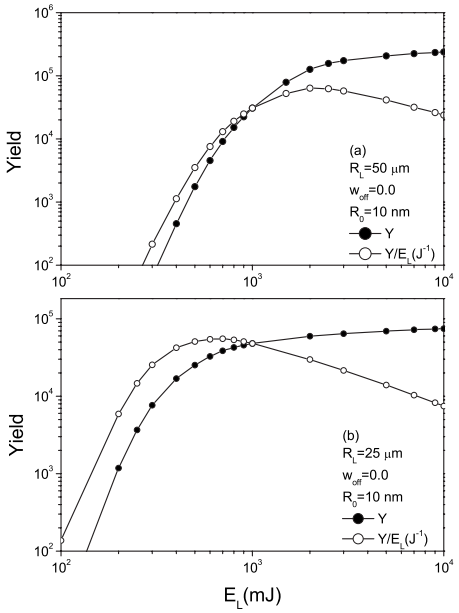

FIG. 5. Fusion yield Y and yield per joule of incident laser energy $Y/E_L(\mathrm{J}^{-1})$ versus initial laser energy E_L for various laser focus position w_{off} and focus radius R_L.

It can be seen from Fig. 5(b) that for the focus radius of 25 μm, the varying trends of the neutron yield and the Y/E_L with the increasing laser energy are similar with those of the laser focal radius 50 μm. The comparison of Fig. 5(a) with Fig. 5(b) indicates that at the point where the fusion yield tends to saturate and Y/E_L starts to decrease, the focus radius of 50 μm allows higher initial laser energy to obtain higher neutron yield and Y/E_L than the laser focus radius of 25 μm. From another view point, a conclusion can be drawn from the relation described above that the higher the initial laser energy is, the broader the focus radius is allowed and the higher the conversion efficiency from the laser energy to

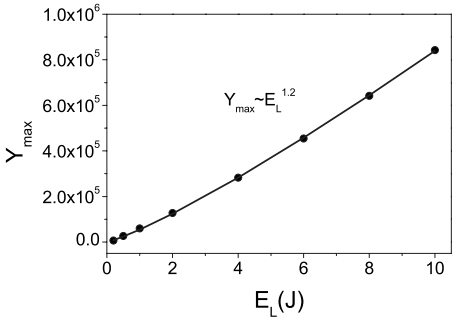

FIG. 6. The maximum fusion yield $Y_{\max}$ as a function of initial laser energy E_L. The solid line represents the least-squares fit of the data points.

the fusion yield is obtained. In fact, this conclusive scaling has already been disclosed in Fig. 3. Therefore, it suggests us that when establishing the experimental scheme, if the increasing laser energy has already led the deuteron energy to saturate, the fusion yield should be expectable to be enhanced with increasing the deuteron number in the interaction volume by use of the broader focus radius.

For different laser energies, the fusion yield can be maximized by use of adjusting the laser focus position and radius. Figure 6 plots the dependence of the maximum neutron yield $Y_{\max}$ on the initial laser energy E_L. It can be seen that the fusion yield roughly increases linearly to the laser energy. As mentioned in the above paragraph, when the laser energy grows higher, it is the broadening focus radius that leads the cluster number to increase in the filament and then maximizes the fusion yield. The power scaling of the maximum fusion yield with the laser energy is $Y_{\max} \sim E_L^{1.2}$, which is different from the reported quantitative relations $Y \sim E_L^{1.6}$ [17] and $Y \sim E_L^{2.2}$ [15] in experiments. The reason originates from the following three factors. Firstly, in experiments it is impossible to test every focus radius while increasing laser energy to determine whether the fusion yield has been maximized with this radius or not. In other words, the yield obtained in the experiments may be not the maximum fusion yield in optimum conditions. Secondly, the increase in the laser energy will lead to the increase in the focus intensity so that the laser intensity beyond the focus spot volume is also high enough to drive the clusters in the additional volume to realize the nuclear fusion. Thirdly, the laser beam with higher energy produces longer cluster filament and then enhances the fusion yield. In our simulation, however, the contribution of clusters in the volume beyond the focus spot to the fusion yield is not considered and the cluster filament length for varying laser energy is estimated to be equal. Due to the latter two factors, the calculated neutron yield for the higher laser energy here is relatively lower and the power parameter in the scaling law of fusion yield with the initial laser energy is smaller than the reported experimental results. The analyses show us a investigating direction for reducing the disparity between the simulations and the experimental measurements.

D. Scaling of fusion yield with cluster size

Figure 7 illustrates the fusion yield Y as a function of the cluster radius R_0 with the given initial laser energy, focus

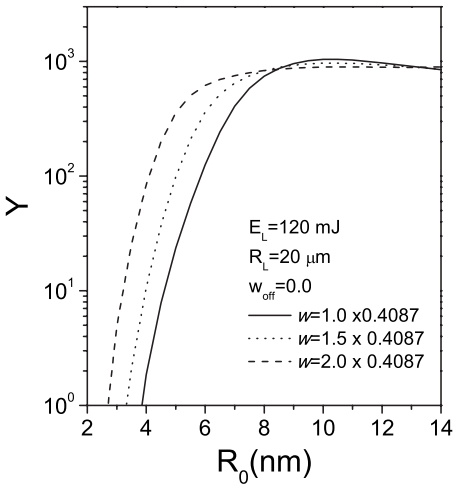

FIG. 7. Cluster radius R_0 dependence of fusion yield Y for different cluster size widths w. The laser pulse has the initial energy 120 mJ and the temporal width 35 fs, same as that used in the experiments of Ref. [15]. The pulse with focus radius 20 μm is focused onto the cluster jet center.

radius, and position. To compare our results with the experimental measurements in Fig. 7 of Ref. [15], the initial energy of the laser pulse is set to be 120 mJ and the temporal width is chosen as 35 fs, same as that used in the experiments [15]. The pulse with the focus spot radius 20 μm that can maximize the total fusion yield for most cluster sizes is focused onto the cluster jet center. At every mean cluster size R_0, we choose three values $w=0.4087$, $w=1.5\times0.4087$, and $w=2\times0.4087$ to investigate the influence of the cluster size width on the neutron yield at the same laser parameters. Here the parameter w refers to the cluster size width appearing in Eq. (6). As represented by solid line of $w=0.4087$, the fusion yield increases with the cluster size rising as long as the cluster radius is smaller than 8 nm. For cluster radius over 8 nm, the fusion yield increases little and then reaches a peak. As the cluster radius continues to increase, the fusion yield appears to have a very slowly decreasing tendency. When the laser parameter is set to be constant, the volume of the cluster filament and correspondingly the rough number of clusters in the filament are almost the same so that it is mainly the deuteron energy generated from the cluster explosion driven by the laser that determines the fusion yield. When the mean cluster radius is relatively small than 4.5 nm, the Coulomb potential accumulated in the clusters is very low, and correspondingly the deuterons with low kinetic energy transferred from the potential only produce low fusion yield below 10. As the radius increases over 5 nm, the deuteron energy is enhanced and then the fusion neutron yield begins to increase sharply. However, the increasing trend will stop when the cluster radius rises to a certain limit. After that limit the laser energy cannot make the outer ionization process of the clusters to finish immediately and the deuteron kinetic energy will have a tendency of falling off. This relation can be seen from this figure, i.e., the fusion yield reaches a peak at the cluster radius of $\sim$10.5 nm and then the yield falls down with the cluster radius increasing. The only possible way to keep the upward tendency of neutron yield with

cluster size is to increase the laser intensity continually to the best.

Moreover, if the cluster size width w broadens (as plotted by dot line and dash line), the neutron yield will increase by a considerable extent as long as the mean cluster radius is smaller than 7 nm. It is because that with the wider size distribution, the clusters that can realize the PCE have higher proportion in the total cluster number of the interaction volume, and then the contribution they made to the fusion yield is also enhanced correspondingly. As the cluster radius increases further, all the neutron yields with different cluster size widths level off at the order of $8\times10^2-1\times10^3$ before beginning to fall slowly. It means that the conversion of the laser energy into the kinetic energy of the deuterons has reached a saturation point. The calculated scaling of the fusion yield with cluster size here is qualitatively in consistence with the measured tendency in Refs. [12,15]. Therefore, it is proposed that we should choose clusters with proper mean size and proper size distribution width for attaining the maximum fusion yield under given laser conditions.

By comparing the results in this figure with the experimental measurements in Fig. 7 of Ref. [15], it is shown that the fusion yields calculated in the simulation are relatively lower than the reported measurements, especially for the small cluster sizes. For example, in our simulation the fusion yield is below 10 for the mean cluster radius 4 nm as shown in Fig. 7, while the measured yield is about 10^2-10^3 in Fig. 7 of Ref. [15]. We make some guesses for the discrepancy as follows. Firstly, based on the analyses whether the cluster can realize the Coulomb explosion under the given laser condition or not, we think that the determination of the mean cluster size in the laser-heated jet plays a key role in investigating the fusion yield variation. Our calculations indicate that only when all the clusters realize the PCE in the interaction volume with the largest radius 100 μm among the laser spot radius range (20–100 μm) presented in Ref. [15] can the fusion yield be improved to maximum 290, close to the measurement value. However, the peak laser intensity corresponding to the laser beam radius 100 μm is $\sim2.0\times10^{16}$ W/cm^2, lower than the critical laser intensity 4.9×10^{16} W/cm^2 for the 4 nm cluster to realize the PCE according to the calculation formula $I_{\mathrm{crit}}(\mathrm{W/cm^2})=8\pi^2c^3m_e\rho R_0^2/3\lambda^2\approx1.94\times10^{15}\,R_0^2(\mathrm{nm})/\lambda^2(\mu\mathrm{m})$ [41]. Even if the laser pulse instantaneously rises to the peak laser intensity $\sim2.0\times10^{16}$ W/cm^2 and the attenuation effect of the laser energy is ignored, the total fusion yield is calculated close to zero, much lower than the measured value. Additionally, considering the laser pulse used in the experiments has the certain width (35 fs) but not reaching the peak intensity in no time, it is obvious that there are more clusters that cannot realize the PCE and the energies of the deuterons are so low that the fusion reactions would hardly occur in the heated cluster plasma. On the other hand, according to the presentation of Ref. [26] the averaged fusion cross section $\langle\sigma\rangle$ increases sharply with the increased ion energy in the low-energy region and finally enhances the neutron yield by several orders, while the ion energy fluctuation is mainly determined by the cluster size variation if the laser characteristic parameters are kept unchanged. Furthermore, the broadening cluster size width for the same mean cluster size will also increase the neutron yield to a great extent. Just as plotted by dash line in Fig. 7, if the cluster size width doubles the fusion yield is improved close to 10^2. Therefore one possible reason for the higher fusion yield in the experiments may be that the cluster jet used in the experiments has the larger mean cluster size than the measured and the jet exhibits a broader size distribution. Secondly, it is implied in Eq. (7) that the fusion yield depends highly on the laser focus spot radius R_L. In Fig. 7 the focus radius R_L is chosen as 20 μm that can maximize the total fusion yield for most cluster sizes; however, the laser focus spot size for Fig. 7 of Ref. [15] is not presented definitely in their paper. The uncertain laser focus spot radius would also lead to the difference in the fusion yield between the reported experiments and our simulations. Thirdly, the volume of the cluster plasma filament is underestimated a little herein in the viewpoints of the physics reality. In experiments, the intensity on the laser spot plane has a Gaussian distribution; as a result, if the laser intensity in the plane boundary beyond the laser spot radius is high enough for the small clusters (e.g., with the mean radius $\sim$4 nm), it will also interact with some clusters in this area to contribute the fusion yield. However this contribution is not considered in our simulations where the statistics of the fusion events are terminated at the laser spot radius. Apart from the uncertainties discussed above, a rough qualitative agreement about the variation tendency of fusion yield with laser-cluster parameters is obtained between our simulations and the reported measurements.

IV. CONCLUSION

By employing a simplified but effective model with consideration of the absorption of laser energy by clusters with a logarithmic-normal size distribution, the nuclear fusion yield inside the generated plasma filament when the intense laser pulses heat up the deuterium cluster jet is calculated with varying laser-cluster parameters. It is found that the neutron yield depends on the laser-cluster parameters such as the cluster size, the laser energy, and the focus spot radius and position. Only if these parameters match with each other can the neutron yield or the neutron conversion efficiency be maximized. Some comparisons of our simulated scalings with the reported measurements have been made and the qualitative agreement is obtained. These qualitative relations could potentially provide theoretical proof for establishing the experimental scheme of the fusion yield generated from the interaction of ultrashort intense laser pulse not only with deuterium clusters but also with deuterated clusters such as deuterated methane clusters.

ACKNOWLEDGMENTS

This work was supported by the Chinese National Natural Science Foundations (Contracts No. 10535070 and No. 10674145), the National Basic Research Program of China (Contract No. 2006CB806000), and the Doctor Foundation of Tianjin Normal University (Contract No. 52LX27).

[1] T. Ditmire, T. Donnelly, A. M. Rubenchik, R. W. Falcone, and M. D. Perry, Phys. Rev. A **53**, 3379 (1996).
[2] J. W. G. Tisch, N. Hay, E. Springate, E. T. Gumbrell, M. H. R. Hutchinson, and J. P. Marangos, Phys. Rev. A **60**, 3076 (1999).
[3] E. Springate, N. N. Hay, J. W. G. Tisch, M. B. Mason, T. Ditmire, J. P. Marangos, and M. H. R. Hutchinson, Phys. Rev. A **61**, 044101 (2000).
[4] V. Kumarappan, M. Krishnamurthy, and D. Mathur, Phys. Rev. A **66**, 033203 (2002).
[5] J. Jha, D. Mathur, and M. Krishnamurthy, Appl. Phys. Lett. **88**, 041107 (2006).
[6] D. R. Symes, M. Hohenberger, A. Henig, and T. Ditmire, Phys. Rev. Lett. **98**, 123401 (2007).
[7] T. Ditmire, R. A. Smith, R. J. Marjoribanks, G. Kulcsar, and M. H. R. Hutchinson, Appl. Phys. Lett. **71**, 166 (1997).
[8] R. C. Issac, G. Vieux, B. Ersfeld, E. Brunetti, S. P. Jamison, J. Gallacher, D. Clark, and D. A. Jaroszynski, Phys. Plasmas **11**, 3491 (2004).
[9] A. S. Moore, K. J. Mendham, D. R. Symes, J. S. Robinson, E. Springate, M. B. Mason, R. A. Smith, J. W. G. Tisch, and J. P. Marangos, Appl. Phys. B: Lasers Opt. **80**, 101 (2005).
[10] F. Dorchies, F. Blasco, C. Bonte, T. Caillaud, C. Fourment, and O. Peyrusse, Phys. Rev. Lett. **100**, 205002 (2008).
[11] T. Ditmire, J. Zweiback, V. P. Yanovsky, T. E. Cowan, G. Hays, and K. B. Wharton, Nature (London) **398**, 489 (1999).
[12] J. Zweiback, R. A. Smith, T. E. Cowan, G. Hays, K. B. Wharton, V. P. Yanovsky, and T. Ditmire, Phys. Rev. Lett. **84**, 2634 (2000).
[13] J. Zweiback, T. E. Cowan, R. A. Smith, J. H. Hartley, R. Howell, C. A. Steinke, G. Hays, K. B. Wharton, J. K. Crane, and T. Ditmire, Phys. Rev. Lett. **85**, 3640 (2000).
[14] J. Zweiback and T. Ditmire, Phys. Plasmas **8**, 4545 (2001).
[15] J. Zweiback, T. E. Cowan, J. H. Hartley, R. Howell, K. B. Wharton, J. K. Crane, V. P. Yanovsky, G. Hays, R. A. Smith, and T. Ditmire, Phys. Plasmas **9**, 3108 (2002).
[16] F. Peano, R. A. Fonseca, J. L. Martins, and L. O. Silva, Phys. Rev. A **73**, 053202 (2006).
[17] K. W. Madison, P. K. Patel, D. Price, A. Edens, M. Allen, T. E. Cowan, and J. Zweiback, Phys. Plasmas **11**, 270 (2004).
[18] F. Buersgens, K. W. Madison, D. R. Symes, R. Hartke, J. Osterhoff, W. Grigsby, G. Dyer, and T. Ditmire, Phys. Rev. E **74**, 016403 (2006).
[19] A. E. Kaplan, B. Y. Dubetsky, and P. L. Shkolnikov, Phys. Rev. Lett. **91**, 143401 (2003).
[20] F. Peano, R. A. Fonseca, and L. O. Silva, Phys. Rev. Lett. **94**, 033401 (2005).
[21] F. Peano, R. A. Fonseca, J. L. Martins, and L. O. Silva, Phys. Rev. A **73**, 053202 (2006).
[22] F. Peano, J. L. Martins, R. A. Fonseca, L. O. Silva, G. Coppa, F. Peinetti, and R. Mulas, Phys. Plasmas **14**, 056704 (2007).
[23] I. Last and J. Jortner, Phys. Rev. A **71**, 063204 (2005).
[24] I. Last and J. Jortner, Phys. Plasmas **14**, 123102 (2007).
[25] I. Last and J. Jortner, Phys. Rev. A **77**, 033201 (2008).
[26] H. Li, J. Liu, C. Wang, G. Ni, C. Kim, R. Li, and Z. Xu, J. Phys. B **40**, 3941 (2007).
[27] G. Grillon, Ph. Balcou, J.-P. Chambaret, D. Hulin, J. Martino, S. Moustaizis, L. Notebaert, M. Pittman, Th. Pussieux, A. Rousse, J.-Ph. Rousseau, S. Sebban, O. Sublemontier, and M. Schmidt, Phys. Rev. Lett. **89**, 065005 (2002).
[28] S. Ter-Avetisyan, M. Schnürer, D. Hilscher, U. Jahnke, D. Hilscher, and U. Jahnke, Phys. Plasmas **12**, 012702 (2005).
[29] I. Last and J. Jortner, Phys. Rev. Lett. **87**, 033401 (2001).
[30] I. Last and J. Jortner, Phys. Rev. A **64**, 063201 (2001).
[31] I. Last and J. Jortner, J. Phys. Chem. A **106**, 10877 (2002).
[32] A. Heidenreich, J. Jortner, and I. Last, Proc. Natl. Acad. Sci. U.S.A. **103**, 10589 (2006).
[33] P. B. Parks, T. E. Cowan, R. B. Stephens, and E. M. Campbell, Phys. Rev. A **63**, 063203 (2001).
[34] J. Davis, G. M. Petrov, and A. L. Velikovich, Phys. Plasmas **13**, 064501 (2006).
[35] S. Karsch, S. Düsterer, H. Schwoerer, F. Ewald, D. Habs, M. Hegelich, G. Pretzler, A. Pukhov, K. Witte, and R. Sauerbrey, Phys. Rev. Lett. **91**, 015001 (2003).
[36] Chen Guang-Long, Lu Hai-Yang, Wang Cheng, Liu Jian-Sheng, Li Ru-Xin, Ni Guo-Quan, and Xu Zhi-Zhan, Chin. Phys. B **17**, 2124 (2008).
[37] I. Last and J. Jortner, Phys. Rev. A **73**, 063201 (2006).
[38] K. J. Mendham, N. Hay, M. B. Mason, J. W. G. Tisch, and J. P. Marangos, Phys. Rev. A **64**, 055201 (2001).
[39] S. Sakabe, S. Shimizu, M. Hashida, S. Sato, T. Tsuyukushi, K. Nishihara, S. Okihara, T. Kagawa, Y. Izawa, K. Imasaki, and T. Iida, Phys. Rev. A **69**, 023203 (2004).
[40] Md. Ranaul Islam, U. Saalmann, and J. M. Rost, Phys. Rev. A **73**, 041201(R) (2006).
[41] H. Li, J. Liu, C. Wang, G. Ni, R. Li, and Z. Xu, Phys. Rev. A **74**, 023201 (2006).
[42] G. Chen, C. Wang, H. Lu, S. Li, J. Liu, G. Ni, R. Li, and Z. Xu, J. Phys. B **40**, 445 (2007).
[43] P. Monot, T. Auguste, L. Lompre, G. Mainfray, and C. Manus, J. Opt. Soc. Am. B **9**, 1579 (1992).
[44] A. J. Mackinnon, M. Borghesi, A. Iwase, M. W. Jones, G. J. Pert, S. Rae, K. Burnett, and O. Willi, Phys. Rev. Lett. **76**, 1473 (1996).
[45] P. Chessa, E. De Wispelaere, F. Dorchies, V. Malka, J. R. Marques, G. Hamoniaux, P. Mora, and F. Amiranoff, Phys. Rev. Lett. **82**, 552 (1999).
[46] T. Tajima, Y. Kishimoto, and M. C. Downer, Phys. Plasmas **6**, 3759 (1999).
[47] I. Alexeev, T. M. Antonsen, K. Y. Kim, and H. M. Milchberg, Phys. Rev. Lett. **90**, 103402 (2003).
[48] T. Caillaud, F. Blasco, C. Bonte, and F. Dorchies, Phys. Plasmas **13**, 033105 (2006).
[49] I. Last and J. Jortner, J. Chem. Phys. **121**, 3030 (2004).
[50] M. Eloy, R. Azambuja, J. T. Mendonca, and R. Bingham, Phys. Plasmas **8**, 1084 (2001).